Int. J. Solids Structures Vol. 28, No. 4, pp. 517–531, 1991
Printed in Great Britain.

0020-7683/91 $3.00 + .00

EXACT TRANSIENT RESULTS FOR PENNY-SHAPED CRACK GROWTH UNDER COMBINED LOADING

L. M. BROCK
Anderson Hall, Department of Engineering Mechanics, College of Engineering, University of Kentucky, Lexington, KY 40506-0046, U.S.A.

(*Received* 24 *April* 1990; *in revised form* 28 *November* 1990)

Abstract—Exact transient solutions are obtained for penny-shaped crack growth in an elastic material. The material is loaded by a general combined tension-in-plane shear/torsion field and, for consistency with the crack shape, the field varies axisymmetrically about the crack center axis. Solution construction is in terms of a general 3D dislocation distribution, and draws on exact results derived previously for 2D plane crack growth. For generality in attacking more complicated problems in the future, the solution method makes no appeal at the outset to axisymmetry, nor to the lack of geometric characteristic length. The general expression for the 3D displacement solution vector is presented, and two important cases worked out. One of these—uniform combined loading—is also examined from the viewpoint of fracture mechanics: It is found that the relative importance of any one of the three fracture modes to the fracture energy rate depends on crack growth rate as well as on the loading itself.

1. INTRODUCTION

As the review by Panasyuk *et al.* (1981) and the work by Fabrikant (1989) demonstrate, analytical studies for a wide variety of static 3D crack problems have been made. For non-static 3D problems, however, the emphasis has been on approximate, time-harmonic, or numerical studies of stationary cracks (Achenbach *et al.*, 1982; Martin and Wickham, 1983; Rosakis *et al.*, 1988; McCarthy and Hayes, 1989). Thus, there are relatively few transient analytical studies of growing 3D cracks.

Nevertheless, several of these are of note: in particular, Willis (1973) has obtained approximate transient solutions for 3D crack growth when no characteristic length exists while, even more recently, Erguven (1985) and Brock (1989) derived exact results for a penny-shaped crack growing at a constant rate in, respectively, a uniform torsion and a uniform tension field.

The aim of the present paper is, therefore, a first-step extension of the work by Brock and Willis: a penny-shaped crack growing at a constant subcritical rate in an unbounded isotropic elastic material is treated. As Fig. 1 illustrates in terms of the Cartesian coordinates $\mathbf{x} = (x_1, x_2, x_3)$, the crack lies in the x_1x_2-plane and grows from a point defect at $\mathbf{x} = 0$. The variable s is time multiplied by the dilatational wave speed, so that c is the dimensionless ratio of crack speed to dilatational wave speed. The loading in the material is appropriate for penny-shaped crack growth: the crack plane is placed in a state of axisymmetrically-varying combined tension, in-plane shear and torsion. Exact transient solutions will be obtained, so that some general physical insight will be possible. It is hoped, moreover, that the exact nature of the solution will suggest methods of treating more general 3D crack problems.

In the next section, the transform solution for a related 3D problem is given and partly inverted. This is subsequently used to construct solutions for the penny-shaped crack problem. It will be noted that the solution process makes no appeals at the outset to either the lack of a characteristic length in the geometry or the problem axisymmetry; these properties will subsequently be invoked when particularly convenient.

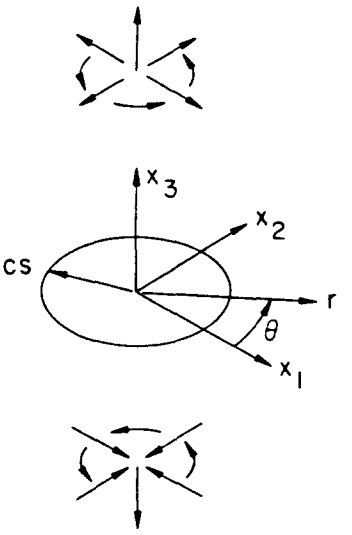

Fig. 1. Geometry of penny-shaped crack growth and combined loading.

2. RELATED 3D PROBLEM

Consider an unbounded, isotropic, linearly elastic material: For $s \leqslant 0$ it is at rest, but for $s > 0$ a dislocation distribution $\mathbf{u}^+ - \mathbf{u}^- = \mathbf{U}$ appears on the finite region A_c of the x_1x_2-plane. Here $(\mathbf{u}, \mathbf{U})$ are the displacement and displacement discontinuity (dislocation) vectors, with Cartesian components (u_i, U_i) $(i = 1, 2, 3)$, while $(\pm)$ denotes evaluation on the surface $x_3 = 0\pm$. The distribution $\mathbf{U} = \mathbf{U}(\mathbf{x}, s)$ is for $s > 0$ continuous and finite in A_c, and vanishes identically outside A_c. The governing equations for the problem are, therefore,

$$\mathbf{u}^+ - \mathbf{u}^- = \mathbf{U} \tag{1a}$$

in A_c for $s > 0$,

$$\mathbf{u} \equiv 0 \tag{1b}$$

for all $\mathbf{x}$ when $s \leqslant 0$ and

$$\nabla^2\mathbf{u} + (m^2 - 1)\nabla(\nabla\cdot\mathbf{u}) = m^2\ddot{\mathbf{u}}, \quad m = v_1/v_2 \tag{2a}$$

$$\frac{1}{\mu}\boldsymbol{\sigma} = (m^2 - 2)(\nabla\cdot\mathbf{u})\mathbf{I} + \nabla\mathbf{u} + \mathbf{u}\nabla \tag{2b}$$

for $s > 0$ and all $\mathbf{x}$ except perhaps A_c. Here ∇ is the gradient operator, $(\dot{})$ denotes s-differentiation, $\boldsymbol{\sigma}$ and $\mathbf{I}$ are the stress and identity tensors, and $(\cdot)$ denotes the inner product. The constants (μ, v_1, v_2) are, respectively, the shear modulus and dilatational and rotational wave speeds. In addition, $\mathbf{u} = \mathbf{u}(\mathbf{x}, s)$ should be continuous along dilatational and rotational wavefronts or, correspondingly, should remain finite as $|\mathbf{x}| \to \infty$ for finite $s > 0$.

To satisfy eqns (1), (2) and the attendant finiteness condition on $\mathbf{u}$, we follow the work of Brock (1986) on a more general dislocation problem: The uni- and bilateral Laplace transforms (Sneddon, 1972)

$$\hat{f}(x) = \int_0^\infty f(\mathbf{x}, s)\, e^{-ps}\, ds, \quad f^*(x_3) = \int\int \hat{f}(\mathbf{x})\, e^{-p(\mathbf{q}\cdot\mathbf{x})}\, dx_1\, dx_2 \tag{3a,b}$$

are applied. Here integration is along the entire Re (x_1, x_2)-axes and the vector $\mathbf{q} = (q_1, q_2, 0)$. The scalar p can be treated as real; in particular, $p > 0$ for this problem. The result is the transform problem

$$(d^2-p^2b^2)\mathbf{u}^*+(m^2-1)(pq_1, pq_2, d)(pq_1u_1^*+pq_2u_2^*+du_3^*)=0 \tag{4a}$$

$$(\mathbf{u}^*)^+-(\mathbf{u}^*)^- = \mathbf{U}^* \tag{4b}$$

for, respectively, $x_3 \neq 0$ and $x_3 = 0$, where $|\mathbf{u}^*|$ must remain finite as $|x_3| \to \infty$. Here

$$a=\sqrt{(1-q^2)}, \quad b=\sqrt{(m^2-q^2)} \tag{5}$$

while d denotes x_3-differentiation and $q = |\mathbf{q}|$. Here $\mathrm{Re}\,(a, b) \geqslant 0$ in the q-plane cut along $\mathrm{Im}\,(q) = 0$, $|\mathrm{Re}\,(q)| > (1, m)$. The appearance of the branch cuts on the $\mathrm{Re}\,(q)$-axis follows from the use of the bilateral Laplace transform, and proves to be of some convenience in manipulating the transform inversions. The wavefront continuity imposed on $\mathbf{u}$, as manifested in the unilateral Laplace transform, can be shown to guarantee the exponentially small behavior at infinity required for the bilateral transform, cf. Brock (1986). The transform problem is readily solved and, in particular, we have for $x_3 = 0$,

$$\frac{2m^2}{\mu p}\sigma_{i3}^* = (q_i^2E-m^2b)U_i^*+q_1q_2EU_{3-i}^* \ (i=1,2), \quad \frac{2m^2}{\mu p}\sigma_{33}^* = -DU_3^* \tag{6a,b}$$

where

$$D=4q^2b+\frac{T^2}{a}, \quad E=\frac{T}{b}+2b-4a, \quad T=m^2-2q^2=b^2-q^2. \tag{7}$$

From Sneddon (1972), the inverse of operation (3b) applied to (6b) gives

$$2(i2m\pi)^2\hat{\sigma}_{33} = -\mu p^3\int\int U_3^*D\,e^{p(\mathbf{q}\cdot\mathbf{x})}\,dq_1\,dq_2 \tag{8}$$

for $x_3 = 0$. We have assumed that $\mathbf{U}^*$ is analytic along the $\mathrm{Im}\,(q_i)$-axes, which are the inversion integration paths in (8). These paths are chosen to avoid the branch cuts of (a, b). Introduction of the rotation

$$\mathbf{q}\cdot\mathbf{x} = Q_1r, \quad Q = q \tag{9}$$

where $r=\sqrt{(x_1^2+x_2^2)}$, $\mathbf{Q} = (Q_1, Q_2, 0)$ and $Q = |\mathbf{Q}|$, produces integration along the $\mathrm{Im}\,(Q_i)$-axes, and an exponential term which is independent of Q_2. Thus, we can write

$$(i2m\pi)^2\hat{\sigma}_{33} = -\mu p^3\int\int (U_3^*)_eD\,e^{pQ_1r}\,dQ_1\,dQ_2 \tag{10}$$

where integration is now along the entire $\mathrm{Im}\,(Q_1)$-axis and the positive $\mathrm{Im}\,(Q_2)$-axis, and the subscript e signifies that part of a function which is even in Q_2. In view of (9),

$$D(q) = D(Q), \quad a(q) = a(Q), \quad b(q) = b(Q), \quad E(q) = E(Q) \tag{11}$$

so that these functions are automatically even in (Q_1, Q_2). Similarly, it can be shown that (6a) yields

$$(i2m\pi)^2\hat{\sigma}_{3i} = \mu p^3\int\int S_{3i}^*\,e^{pQ_1r}\,dQ_1\,dQ_2 \quad (i=1,2) \tag{12a}$$

$$S_{3i}^* = (U_i^*)_e[(Q_i^2\cos^2\theta+Q_{3-i}^2\sin^2\theta)E-m^2b]-(U_{3-i}^*)_oQ_1Q_2E\cos 2\theta$$
$$+[\tfrac{1}{2}(U_{3-i}^*)_e(Q_1^2-Q_2^2)+(-1)^{3-i}(U_i^*)_oQ_1Q_2]E\sin 2\theta \tag{12b}$$

where the subscript o denotes that part of a function which is odd in Q_2. As seen in Fig. 1, (r,θ) are the polar coordinates in the x_1x_2-plane, where $\theta = \tan^{-1}(x_2/x_1)$. Indeed, the complicated nature of (12b) suggests that (r,θ) be used in place of (x_1,x_2). It is then easily shown that (10) remains the same, but that (12) can be replaced by

$$(i2m\pi)^2\hat{\sigma}_{3r} = \mu p^3 \int\int [(U_r^*)_e(Q_1^2E - m^2b) - (U_\theta^*)_o Q_1Q_2E]\, e^{pQ_1r}\, dQ_1\, dQ_2 \qquad (13a)$$

$$(i2m\pi)^2\hat{\sigma}_{3\theta} = \mu p^3 \int\int [(U_\theta^*)_e(Q_1^2E - m^2b) - (U_r^*)_o Q_1Q_2E]\, e^{pQ_1r}\, dQ_1\, dQ_2 \qquad (13b)$$

where now $\mathbf{U} = (U_r, U_\theta, U_3)$. These results are now applied to the penny-shaped crack problem.

3. TRANSFORM ADAPTATION FOR PENNY-SHAPED CRACK PROBLEM

We choose A_1 to be the growing circle $r < cs$ shown in Fig. 1, and $\mathbf{U}$ to represent the relative displacement of the two crack surfaces. For subcritical crack speed,

$$c < c_R \qquad (14)$$

where $c_R < 1/m$ is the Rayleigh wave speed non-dimensionalized with respect to c_1. The crack problem can now be viewed as the superposition of the solution which would exist if no crack were present, and the solution to the problem considered above. Of course, $\mathbf{U}$ must now be chosen so that it vanishes continuously at $r = cs$, while simultaneously cancelling the tractions imposed over A_1 by the first solution.

The first solution represents the loading in the unbounded material. As noted at the outset, this loading produces an axisymmetrically-varying tension shear torsion field on the crack plane. We here assume that this field can be represented by polynomials in (r,s). Clearly, the terms in these polynomials can be grouped according to their degree of homogeneity n (Brock, 1976) so that, by superposition, the traction field imposed on $x_3 = 0$ can be written as combinations of the sets

$$\mathbf{e}_3\cdot\boldsymbol{\sigma} = s^n\mathbf{B}_n(\xi), \quad \xi = \frac{r}{s}. \qquad (15a,b)$$

Here $\mathbf{e}_3$ is the x_3-basis vector, $\boldsymbol{\sigma}$ is now in the coordinates (r,θ,x_3) and the components of the vector $\mathbf{B}_n$ are linear combinations of powers of ξ between 0 and n. For present purposes, it suffices to consider $n \geqslant 0$.

By superposition, a field $\mathbf{U}$ can be obtained separately for each given traction set (15a). Because the problem geometry exhibits no characteristic length, this $\mathbf{U}$ will be homogeneous of degree $n+1$ in (r,s) (Achenbach and Brock, 1971; Brock, 1978). Therefore,

$$\mathbf{U} = s^{n+1}\int_c^{\infty} (t-\xi)^{n+1}\mathbf{A}(t)\, dt, \quad r \leqslant cs \qquad (16)$$

is an appropriate candidate, where the vector distribution $\mathbf{A}(t)$ over the dimensionless, speed-related parameter t is now the quantity sought.

In view of (10) and (13), the double transform of (16) is required: Application of (3), changing the integration variables from (x_1,x_2) to (r,θ) and then interchanging the order of (r,s) integration gives a form in which both these integrations can be performed. The result is

$$\mathbf{U}^* = \frac{(n+1)!}{p^{n+3}} \int_0^c t^{n-1} \int_0^{2\pi} \frac{\mathrm{d}\theta}{(k+q_1\cos\theta+q_2\sin\theta)^2} \mathbf{A}(t)\,\mathrm{d}t, \quad k = \frac{1}{t}. \tag{17a,b}$$

The θ-integration can be written as $-\partial I/\partial k$, where

$$I = \int_0^{2\pi} \frac{\mathrm{d}\theta}{k+q_1\cos\theta+q_2\sin\theta}. \tag{18}$$

For q real, (18) can be performed by use of standard tables (Peirce and Foster, 1957) to give

$$I = \frac{2\pi}{\sqrt{(k^2-q^2)}}, \quad k \geqslant q,$$

whereupon, in view of (9), (17a) becomes

$$\mathbf{U}^* = (\mathbf{U}^*)_r = 2\pi \frac{(n+1)!}{p^{n+4}} \int_0^c \frac{t^n}{\sqrt{(k^2-Q^2)^3}} \mathbf{A}(t)\,\mathrm{d}t, \quad k \geqslant Q. \tag{19}$$

Upon substitution of (19) and making the imaginary nature of Q_2 explicit, i.e. $Q_2 = iu$ (u real), (10) gives

$$i2\pi m^2 \hat{\sigma}_{33} = -\mu(n+1)! \int_0^c \left(\frac{t}{p}\right)^n A_3(t) \iint \frac{D}{\sqrt{(C^2-Q_1^2)^3}} \mathrm{e}^{pQ_1 r}\,\mathrm{d}Q_1\,\mathrm{d}u\,\mathrm{d}t \tag{20}$$

where $\mathbf{A} = (A_r, A_\theta, A_3)$, integration is now along the positive $\mathrm{Re}\,(u)$- and entire $\mathrm{Im}\,(Q_1)$-axes, and

$$Q^2 = Q_1^2 - u^2, \qquad a = \sqrt{(I^2-Q_1^2)}, \quad b = \sqrt{(M^2-Q_1^2)} \tag{21a}$$

$$I = \sqrt{(1+u^2)}, \quad M = \sqrt{(m^2+u^2)}, \quad C = \sqrt{(k^2+u^2)}. \tag{21b}$$

It is noted in view of (7) that the integrand of (20) exhibits the branch cuts $\mathrm{Im}\,(Q_1) = 0$ and, respectively, $(I, M) < |\mathrm{Re}\,(Q_1)| < C$. Neither function has poles in its cut Q_1-plane, and both vanish exponentially as $|Q_1| \to \infty$, $\mathrm{Re}\,(Q_1) < 0$. Therefore, by the Cauchy theorem, the Q_1-integration can be deformed onto contours around the branch cuts on the negative $\mathrm{Re}\,(Q_1)$-axis. The result is

$$\pi m^2 \hat{\sigma}_{33} = \mu(n+1)! \int_0^c \left(\frac{t}{p}\right)^n A_3(t) \int_0^t \left(\int_M^C 4Q^2 b - \int_I^C \frac{T^2}{a} \right) \frac{\mathrm{e}^{-pwr}}{\sqrt{(C^2-w^2)^3}} \mathrm{d}w\,\mathrm{d}u\,\mathrm{d}t \tag{22}$$

where $-w$ replaces Q_1 and now

$$Q^2 = w^2 - u^2, \quad a = \sqrt{(w^2-I^2)}, \quad b = \sqrt{(w^2-M^2)}. \tag{23}$$

Similar expressions can be obtained from (13) for $(\hat{\sigma}_{3r}, \hat{\sigma}_{30})$. In the next section, the inversion of all these transforms is completed.

4. TRANSFORM INVERSION

By inspection, the inverse unilateral Laplace transform of the p-dependent terms in (22) is

$$\frac{1}{n!}(s-wr)^n H(s-wr) \tag{24}$$

where $H(\ )$ is the Heaviside function. If we assume that the operations of (u, w, t)-integration and inversion can be interchanged, then (22) and (24) give

$$\frac{\pi m^2}{\mu(n+1)!}\sigma_{33} = \int_0^c A_3(t)\frac{t^n}{\sqrt{(k^2-v^2)^3}}\left(\int_m^L 4v^2 b - \int_1^L \frac{T^2}{a}\right)X_n\,\mathrm{d}v\,\mathrm{d}t, \quad \tau = \frac{s}{r} \tag{25}$$

for $x_3 = 0$. Here $L = \min(k, \tau)$, the (u, w)-integration orders have been interchanged, and the integration variable change $w = \sqrt{(u^2+v^2)}$ made, i.e.

$$Q = v, \quad a = \sqrt{(v^2-1)}, \quad b = \sqrt{(v^2-m^2)}, \quad T = m^2-2v^2. \tag{26}$$

The function X_n is defined as

$$X_n = \int_0^{\sqrt{(\tau^2-v^2)}} [\tau - \sqrt{(u^2+v^2)}]^n \frac{\mathrm{d}u}{\sqrt{(u^2+v^2)}}. \tag{27}$$

In view of (15b) and Fig. 1, it is more convenient to use the dimensionless variable ξ, and to eliminate the need for the symbol k. Therefore, the integration variable change $v = 1/z$ is introduced in (25), and it can then be shown that

$$\frac{\pi m^2}{\mu(n+1)!}\sigma_{33} = r^n \int_0^c A_3(t)\frac{t^{n+1}}{\sqrt{(z^2-t^2)^3}}\left(\int_{1/m}^{1} S_B + \int_1^t S_A\right)\Psi_n\left(\frac{z}{\xi}\right)\frac{\mathrm{d}z}{z^{n+4}}\,\mathrm{d}t \tag{28}$$

for $x_3 = 0$. Now $L = \max(c, \xi)$ and

$$\alpha S_A = -N^2, \quad S_B = 4\beta, \quad \alpha = \sqrt{(1-z^2)}, \quad \beta = \sqrt{(1-m^2z^2)}, \quad N = 2-m^2z^2 \tag{29}$$

$$\Psi_0(x) = ch^{-1}x, \quad \Psi_n(x) = \int_1^x (x-u)^{n-1}\Psi_0(u)\,\mathrm{d}u \quad (n \geqslant 1) \tag{30}$$

and z-integration is along the upper side of the Re(z)-axis. It should be noted that the integrations in (30) can, if needed, be performed by standard tables (Peirce and Foster, 1957).

In view of (15a), $\mathbf{A}(t)$ must be chosen so that (28) gives a polynomial homogeneous of degree n in (r, s) when $r < cs(\xi < c)$. An analogous requirement arises in the treatment of 2D plane crack extension under polynomial-form loading (Brock, 1978). Indeed the 2D results suggest the trial form

$$\mathbf{A}(t) = \sum \mathbf{a}_i \frac{t^{2i-n}}{\sqrt{(c^2-t^2)^{2i+3}}} \tag{31}$$

where the vectors $\mathbf{a}_i = (a_{i1}, a_{i0}, a_{i3})$ are arbitrary constants and summation is over i from 0 to n. It is noted that the number of unknown coefficients, $3(n+1)$, is equal to the number of coefficients needed to completely define the vector polynomial $\mathbf{B}_n$. Equation (16) thus becomes

$$\mathbf{U} = s^{n+1}\sum \mathbf{a}_i \int_\xi^c (t-\xi)^{n+1}\frac{t^{2i-n}}{\sqrt{(c^2-t^2)^{2i+3}}}\mathrm{d}t, \quad r \leqslant cs. \tag{32}$$

Despite the singular upper limit, (32) can readily be evaluated to give a finite result, by

interpreting it as a finite part integral (Hadamard, 1908). For example, when $n = 0$ we can write

$$\mathbf{U} = s\mathbf{a}_0\left(\int_0^c - \int_0^r\right)\frac{t-\xi}{\sqrt{(c^2-t^2)^3}}\,dt. \tag{33}$$

The first integral is written as the real part of an integration along the upper side of the entire positive $\mathrm{Re}(t)$-axis. The Cauchy theorem is then used to change the path onto the positive $\mathrm{Im}(t)$-axis, where the integration is easily shown to give $-1/c$. Standard tables can be used to evaluate the integration from 0 to ξ. The result is

$$\mathbf{U} = -\mathbf{a}_0\frac{s}{c^2}\sqrt{(c^2-\xi^2)}, \quad r \leqslant cs. \tag{34}$$

Substitution of (31) into (28) and interchange of the (t,z)-integrations yields two t-integrations which can be performed by use of the Cauchy theorem. Indeed, the two integrations give the same result, so that (28) becomes

$$\frac{\pi m^2}{c\mu(n+1)!}\sigma_{xy} = r^n\sum a_{ir}c_i\left(\int_z^{1/m} S_B + \int_z^1 S_A\right)\Psi_n\left(\frac{z}{\xi}\right)G_m(z,c)\,dz \tag{35}$$

for $x_3 = 0$, where

$$c_0 = -2, \quad c_i = -\frac{2(i+1)}{2i+1}c_{i-1}\ (i \geqslant 1), \quad G_m(x,c) = \frac{x^{2m-2}}{(x^2-c^2)^{m+1/2}}. \tag{36}$$

By a similar process, we obtain

$$\frac{2\pi m^2}{c\mu(n+1)!}\sigma_{yz} = r^n\sum a_{ir}c_i\int_z^{1/m}\left[T_B\Psi_n\left(\frac{z}{\xi}\right) + U_B\Omega_n\left(\frac{z}{\xi}\right)\right]G_m(z,c)\,dz$$
$$+ r^n\sum a_{ir}c_i\int_z^1\left[T_A\Psi_n\left(\frac{z}{\xi}\right) + U_A\Omega_n\left(\frac{z}{\xi}\right)\right]G_m(z,c)\,dz \tag{37}$$

for $x_3 = 0$, where σ_{xz} follows by replacing (T_A, T_B) with their negatives, and a_{ir} with a_{im}. In (37)

$$T_A = U_A = 4\alpha, \quad U_B = 2m^2z^2\beta + T_B, \quad \beta T_B = m^2z^2 - 2N \tag{38}$$

while

$$\Omega_0(x) = x\sqrt{(x^2-1)}, \quad \Omega_n(x) = \int_1^x (x-u)^{n-1}\Omega_0(u)\,du\ (n \geqslant 1). \tag{39}$$

As with Ψ_n, the integrations in (39) can easily be performed if needed.

The tractions generated on $x_3 = 0$ by $\mathbf{U} \neq \mathbf{0}$ defined over the zone $r < cs$ will travel as dilatational and rotational waves. Because these waves exist in, respectively, the regions $r < s(\xi < 1)$ and $r < s/m(\xi < 1/m)$, they can immediately be identified as the A- and B-subscripted terms in (35) and (37).

Although the forms of these equations suggest otherwise, two examples now considered will demonstrate that (35) and (37) do indeed behave as polynomials of degree n in (r,s) when $r < cs$, thus allowing the problem solutions to be completed.

5. VARYING PURE TENSION

If we consider the unbounded material subjected to pure tension, then $\mathbf{B}_n = (0, 0, B_{n3})$ in (15a), whereupon (37) and its $\sigma_{3\theta}$-counterpart show that

$$(a_{ir}, a_{i\theta}) = 0. \tag{40}$$

That is, $\mathbf{U} = (0, 0, U_3)$ in (32). To illustrate how to obtain the a_{i3} for U_3, we consider the case $n = 2$. Then (15a) gives the general form

$$\sigma_{33} = s^2(b_0 + b_1\xi + b_2\xi^2) = b_0 s^2 + b_1 rs + b_2 r^2 \tag{41}$$

for $x_3 = 0$, $r < cs$, where the b_i are specified positive constants. For $r < cs$, $n = 2$, it can be shown that (35) can be written as

$$\frac{\pi m^2}{6\mu}\sigma_{33} = cr^2 \sum a_{i3} c_i \operatorname{Im} \int_0^c \Delta\Psi_2\left(\frac{z}{\xi}\right) G_{2i}(z, c)\, dz + \frac{3\pi}{2c^3}(m^2 - 1) a_{03} rs \tag{42}$$

where (15b) has been used,

$$\Delta = 4B + \frac{N^2}{A}, \quad B = \sqrt{(m^2 z^2 - 1)}, \quad A = \sqrt{(z^2 - 1)} \tag{43}$$

and integration is along the upper ($\operatorname{Im}(z) = 0+$) side of the z-axis. In (42), integrand terms involving (A, B) have branch cuts along $\operatorname{Im}(z) = 0$, $\xi < |\operatorname{Re}(z)| < (1, 1/m)$, respectively. The singularity at $z = c$ in G_{2i} lies, therefore, on the integrand branch cuts. However, (30) shows that

$$4\Psi_2\left(\frac{z}{\xi}\right) = 3i\frac{z}{\xi}\sqrt{\left[1 - \left(\frac{z}{\xi}\right)^2\right]} + i\left[1 + 2\left(\frac{z}{\xi}\right)^2\right]\theta_1\left(\frac{\xi}{z}\right), \quad \theta_1(x) = \tan^{-1}\sqrt{(x^2 - 1)} \tag{44}$$

for $\operatorname{Im}(z) = 0+$, $|\operatorname{Re}(z)| < \xi$, thus allowing a pole to exist at $z = 0$ for the a_{0i}-term; the additional term in (42) corrects for the residue of this pole. The integrand has no other poles or branch cuts in the first quadrant of the z-plane, and behaves no worse than $O(z^{-2})$ when $|z| \to \infty$. The Cauchy theorem can be used, therefore, to transform the integration path in (42) onto the positive $\operatorname{Im}(z)$-axis, where (30) becomes

$$4\Psi_2\left(\frac{z}{\xi}\right) = -3\frac{v}{\xi}\sqrt{\left[1 + \left(\frac{v}{\xi}\right)^2\right]} + \left[1 - 2\left(\frac{v}{\xi}\right)^2\right]\left(\ln\left[\frac{v}{\xi} + \sqrt{\left[1 + \left(\frac{v}{\xi}\right)^2\right]}\right] + i\frac{\pi}{2}\right), \quad z = iv\ (v > 0). \tag{45}$$

Then, taking the imaginary part of the integral in view of (15b) and (36), (43) and (45) gives

$$\frac{m^2}{3\mu}\sigma_{33} = \frac{c}{4}\sum a_{i3} c_i \int_0^c \frac{R_1 v^{2(i-2)}}{(v^2 + c^2)^{i+2}}(2v^2 s^2 - r^2)\, dv + \frac{3}{c^3}(m^2 - 1) a_{03} rs \tag{46}$$

where

$$R_1 = 4b_1 - \frac{1}{a_1}(2 + m^2 v^2)^2, \quad a_1 = \sqrt{(1 + v^2)}, \quad b_1 = \sqrt{(1 + m^2 v^2)} \tag{47}$$

and it should be noted that the v-integrations can be expressed in terms of complete elliptic

integrals (Gradshteyn and Ryzhik, 1980). For purposes of analysis and computation, however, the forms given in (46) are actually more efficient.

Equation (46) is clearly a polynomial homogeneous of degree 2 in (r, s). Thus, setting it equal to the negative of (41) gives a set of three linear equations for the unknown coefficients (a_{03}, a_{13}, a_{23}) in terms of the specified constants (b_0, b_1, b_2). The crack problem is, therefore, essentially solved.

We must consider a case in which all three traction components must be removed.

6. UNIFORM TENSION, SHEAR AND TORSION

For the case of uniform tension, shear and torsion, $n = 0$ and (15a) can be written as

$$\mathbf{e}_3 \cdot \boldsymbol{\sigma} = \mathbf{B}_0 = \mathbf{b} \tag{48}$$

where the components (b_r, b_θ, b_3) of $\mathbf{b}$ are specified positive constants. For $n = 0$ it is easily shown in view of (36) that (35) and (37) give for $x_3 = 0$, $r < cs$,

$$\pi m^2 \sigma_{33} = -2\mu c a_{03} \operatorname{Im} \int_0^r \Delta\Psi_0\left(\frac{z}{\xi}\right) \frac{\mathrm{d}z}{z^2(z^2 - c^2)^2} \tag{49a}$$

$$\pi m^2 \sigma_{3r} = -2\mu c a_{0r} \operatorname{Im} \int_0^r \left[\Delta_\Psi \Psi_0\left(\frac{z}{\xi}\right) + \Delta_\Omega \Omega_0\left(\frac{z}{\xi}\right)\right] \frac{\mathrm{d}z}{z^2(z^2 - c^2)^2} \tag{49b}$$

while $\sigma_{3\theta}$ follows from (49b) by replacing a_{0r} with $a_{0\theta}$ and Δ_Ω with $-\Delta_\Omega$. Here

$$\Delta_\Psi = 4A + 2m^2 c^2 B + \frac{1}{B}(2N - m^2 c^2), \quad \Delta_\Omega = 4A + \frac{1}{B}(2N - m^2 c^2) \tag{50}$$

and the integrand branch cuts are the same as they were for (42), but it is noted that no poles exist in the cut z-plane for this case. The Cauchy theorem can yet again be used to change the integration paths onto the positive $\operatorname{Im}(z)$-axis, where (30) and (39) reduce to

$$\Psi_0\left(\frac{z}{\xi}\right) = \ln\left[\frac{v}{\xi} + \sqrt{\left[1 + \left(\frac{v}{\xi}\right)^2\right]}\right] + i\frac{\pi}{2}, \quad \Omega_0\left(\frac{z}{\xi}\right) = -\frac{v}{\xi}\sqrt{\left[1 + \left(\frac{v}{\xi}\right)^2\right]}, \quad z = iv \ (v > 0). \tag{51}$$

In view of (51), it can then be shown that (49) and their $\sigma_{3\theta}$-counterpart give the constants

$$\sigma_{33} = -\mu c \frac{\Phi_1}{m^2} a_{03}, \quad (\sigma_{3r}, \sigma_{3\theta}) = -\mu c \frac{\Phi_2}{2m^2}(a_{0r}, a_{0\theta}) \tag{52}$$

for $x_3 = 0$, $r < cs$, where

$$\Phi_i = \int_0^r \frac{R_i \, \mathrm{d}v}{v^2(v^2 + c^2)^2} < 0, \quad R_2 = 4a_1 - 2m^2 v^2 b_1 - \frac{1}{b_1}(4 + 3m^2 v^2) \tag{53}$$

and R_1 is given by (47). As with (46), the integrals Φ_i can be expressed in terms of complete elliptic integrals, although their present forms are actually more convenient. Setting (52) equal to the negative of (48) yields

$$a_{03} = \frac{m^2}{\mu c \Phi_1} b_3, \quad (a_{0r}, a_{0\theta}) = \frac{2m^2}{\mu c \Phi_2}(b_r, b_\theta) \tag{54}$$

which completes the solution process. With the validity of (31) and the method for determining the coefficients $\mathbf{a}_i$ demonstrated, we now present general results for the displacement field generated in $x_3 > 0$ by the traction removal process.

7. GENERAL EXPRESSIONS FOR TRACTION REMOVAL SOLUTION

Returning to the original transform problem associated with (4), it is easily shown that for $x_3 > 0$,

$$2m^2 u_i^* = q_i\left(2\omega^* - \frac{T}{a}U_3^*\right)e^{-pax_3} + (m^2 U_i^* - 2q_i\omega^* + 2q_i b U_3^*)\,e^{-pbx_3} \quad (i = 1, 2) \tag{55a}$$

$$2m^2 u_3^* = (TU_3^* - 2a\omega^*)\,e^{-pax_3} + \left(2q^2 U_3^* + \frac{T}{b}\omega^*\right)e^{-pbx_3} \tag{55b}$$

$$\omega^* = q_1 U_1^* + q_2 U_2^* \tag{55c}$$

where (a, b, t) are given by (5) and (7). As before, it is convenient to employ the coordinates (r, θ, x_3). Therefore, we apply the inverse of (3b), and introduce both the new coordinates and the rotation (9). The result is

$$(i2m\pi)^2 \hat{\mathbf{u}} = n! p^2 \iint e^{pQ_1 r}(\mathbf{M}_1 e^{-pax_3} + \mathbf{M}_B e^{-pbx_3})\,dQ_1\,dQ_2 \tag{56}$$

where now $\mathbf{u} = (u_r, u_\theta, u_3)$, and the (r, θ, x_3)-components of the $\mathbf{M}$-vectors are

$$\mathbf{M}_{1r} = 2Q_1^2(U_r^*)_e - 2Q_1 Q_2(U_\theta^*)_o - Q_1\frac{T}{a}(U_3^*)_e \tag{57a}$$

$$\mathbf{M}_{1\theta} = -2Q_1 Q_2(U_r^*)_o + 2Q_1^2(U_\theta^*)_e + Q_2\frac{T}{a}(U_3^*)_o \tag{57b}$$

$$\mathbf{M}_{13} = -2aQ_1(U_r^*)_e + 2aQ_2(U_\theta^*)_o + T(U_3^*)_e \tag{57c}$$

$$\mathbf{M}_{Br} = (m^2 - 2Q_1^2)(U_r^*)_e + 2Q_1 Q_2(U_\theta^*)_o + 2Q_1 b(U_3^*)_e \tag{57d}$$

$$\mathbf{M}_{B\theta} = 2Q_1 Q_2(U_r^*)_o + (m^2 - 2Q_2^2)(U_\theta^*)_e - 2Q_2 b(U_3^*)_o \tag{57e}$$

$$\mathbf{M}_{B3} = Q_1\frac{T}{b}(U_r^*)_e + Q_2\frac{T}{b}(U_\theta^*)_o + 2Q^2(U_3^*)_e. \tag{57f}$$

Integration is, as in (10) and (13), along the entire $\mathrm{Im}\,(Q_1)$-axis and positive $\mathrm{Im}\,(Q_2)$-axis. At this point, the forms (19) and (31) are introduced, and formal integration yields

$$\mathbf{U}^* = (\mathbf{U}^*)_e = 2\pi c\,\frac{(n+1)!}{p^{n+4}}\sum \mathbf{a}_i \frac{c_i}{(1 - c^2 Q^2)^{i+2}}. \tag{58}$$

Again, it is useful to make the imaginary nature of Q_2 in (56) explicit by writing $Q_2 = iu$ (u real), but we now change the Q_1-integrations onto paths in the cut Q_1-plane along which the exponential terms assume the form e^{-pv}, where v is real and positive. These are, of course, the Cagniard–deHoop contours (deHoop, 1960) given by

$$p^2 Q_1 = -vr \pm ix_3\sqrt{(v^2 - I^2\rho^2)}\,(v \geqslant I\rho), \quad p^2 Q_1 = -vr \pm ix_3\sqrt{(v^2 - M^2\rho^2)}\,(v \geqslant M\rho) \tag{59}$$

for the $(\mathbf{M}_A, \mathbf{M}_B)$-terms, respectively, where (I, M) are given by (21b) while $\rho = |x|$. The two contours are branches of hyperbolae in the left half of the Q_1-plane, with $\mathrm{Re}(Q_1)$-axis intercepts at $Q_1 = (-Ir/\rho, -Mr/\rho)$, respectively. It is noted that neither intercept lies on the branch cuts of its corresponding integrand. For $x_3 = 0$, of course, these contours collapse into the paths used in obtaining (22). The inverse of the p-terms can now be obtained by inspection, cf. (24), as

$$\frac{1}{(n+1)!}(s-t)^{n+1}H(s-t) \tag{60}$$

whereupon, from (56) and (59) it is easy to show that

$$\pi m^2 \mathbf{u} = c\sum c_i \int_\nu^s (s-t)^{n+1} \operatorname{Im} \int_0^{\sqrt{(t^2\rho^2-1)}} \frac{\mathbf{m}_{Ai}}{\sqrt{(t^2-I^2\rho^2)}} \frac{\mathrm{d}u}{(1-c^2Q^2)^{i+2}} \mathrm{d}t$$

$$+ c\sum c_i \int_{m\rho}^s (s-t)^{n+1} \operatorname{Im} \int_0^{\sqrt{(t^2\rho^2-m^2)}} \frac{\mathbf{m}_{Bi}}{\sqrt{(t^2-M^2\rho^2)}} \frac{\mathrm{d}u}{(1-c^2Q^2)^{i+2}} \mathrm{d}t. \tag{61}$$

The $(+)$-sign is chosen in (59) and, from (57),

$$\mathbf{m}_{Ai} = \left(2Q_1^2 a_{ir} - Q_1 \frac{T}{a} a_{i3}, \quad -2u^2 a_{i\theta}, \quad -2aQ_1 a_{ir} + T a_{i3}\right) \tag{62a}$$

$$\mathbf{m}_{Bi} = \left[(m^2 - 2Q_1^2)a_{ir} + 2Q_1 b a_{i3}, \quad (m^2+2u^2)a_{i\theta}, \quad Q_1 \frac{T}{b} a_{ir} + 2(Q_1^2+u^2)a_{i3}\right]. \tag{62b}$$

An alternative form more closely related to those derived previously for $x_3 = 0$ can be obtained by introducing the integration variables (w, z), where $w = \rho/t$ and, for the $(\mathbf{m}_{Ai}, \mathbf{m}_{Bi})$-terms, $z = (1/I, 1/M)$, respectively. The result is

$$\pi m^2 \mathbf{u} = cs^{n+1} \sum c_i \rho^{2i+1} \int_\xi^1 \frac{z^{2i}}{\alpha} \operatorname{Im} \int_\xi^z F_{Ai} \mathbf{m}_{Ai} \, \mathrm{d}w \, \mathrm{d}z$$

$$+ cs^{n+1} \sum c_i \rho^{2i+1} \int_\xi^{1,m} \frac{z^{2i}}{\beta} \operatorname{Im} \int_\xi^z \mathrm{F}_{Bi} \mathbf{m}_{Bi} \, \mathrm{d}w \, \mathrm{d}z, \quad \xi = \frac{\rho}{s} \tag{63}$$

for $x_3 > 0$, where (α, β, n) are defined by (29),

$$F_{Ai} = \frac{(w-\xi)^{n+1}}{(Z^2 - c^2 W_A)^{i+2}} \frac{w^{2i}}{\sqrt{(z^2-w^2)}}, \quad Z = \rho z w \tag{64a}$$

$$W_A = W^2 - \rho^2 w^2 \alpha^2, \quad W_B = W^2 - \rho^2 w^2 \beta^2, \quad W = -zr + ix_3\sqrt{(z^2-w^2)} \tag{64b}$$

and

$$\mathbf{m}_{Ai} = \left[\frac{WP_A}{\sqrt{(z^2-w^2)}} a_{i3} - 2W^2 W' a_{ir}, \quad 2(\rho w)^2 \alpha^2 W' a_{i\theta}, \right.$$

$$\left. \frac{2W}{\sqrt{(z^2-w^2)}}(Z^2 - W_A)a_{ir} - P_A W' a_{i3}\right] \tag{65a}$$

$$(m_{Bi})_r = (2W^2 - m^2 Z^2)W' a_{ir} + 2W(W_B - m^2 Z^2)a_{i3} \tag{65b}$$

$$(m_{Bi})_\theta = -(\rho w)^2 N W' a_{i\theta} \tag{65c}$$

$$(m_{Bl})_3 = -\frac{WP_B}{\sqrt{(z^2-w^2)}}a_{lr} - 2W_B W' a_{l3}. \tag{65d}$$

In (63)–(65)

$$W' = ir + x_3\frac{z}{\sqrt{(z^2-w^2)}}, \quad P_A = -2W'^2 + (\rho w)^2(2-N), \quad P_B = -2W'^2 + (\rho w)^2 N. \tag{66}$$

Despite their formidable appearance, the w-integrations in (63) can be performed. In particular, the highly-singular (F_{A0}, F_{B0})-terms can be treated in the same manner indicated by (33). However, like their counterparts defined in (30) and (39), the present forms are more convenient.

In both (61) and (63), the partial uncoupling of the crack surface relative displacements previously noted for the $x_3 = 0$ tractions is also evident: in particular, the tangential (θ) component, which represents relative slip in torsion, affects only the tangential displacement for all $x_3 > 0$. Moreover, the dilatational and rotational wave components are clearly those terms with, respectively, subscripts A and B.

To conclude this analysis, we now examine some fracture mechanics aspects in terms of the uniform traction case solution outlined earlier.

8. FRACTURE MECHANICS ASPECTS FOR UNIFORM TRACTION CASE

From a fracture mechanics viewpoint, the tractions generated just ahead of the crack edge $(x_3 = 0, r = cs+)$ are of particular interest. Returning now to (35) and (37), we find in view of (36) that for $x_3 = 0$, $cs < r < s/m (c < \xi < 1/m)$ the singularity at $z = c$ now lies off of the integrand branch cuts $\mathrm{Im}(z) = 0$, $\xi < |\mathrm{Re}(z)| < (1, 1/m)$. This singularity is of order 2, and we note that (30) and (39) give

$$\Psi_0\left(\frac{z}{\xi}\right) = i\theta_1\left(\frac{\xi}{z}\right), \quad \Omega_0\left(\frac{z}{\xi}\right) = -i\frac{z}{\xi}\sqrt{\left[1-\left(\frac{z}{\xi}\right)^2\right]} \tag{67}$$

for $\mathrm{Im}(z) = 0^+$, $|\mathrm{Re}(z)| < \xi$. These observations, along with the convenient form of (49), suggest that for $x_3 = 0$, $c < \xi < 1/m$ we can write

$$\pi m^2 \sigma_{33} = -\mu a_{03}\frac{\partial}{\partial c}\left[\mathrm{Im}\int_0^{\infty}\Delta\Psi_0\left(\frac{z}{\xi}\right)\frac{\mathrm{d}z}{z^2(z^2-c^2)} - \frac{\pi}{2}\frac{R}{c^3\chi}\theta_1\left(\frac{\xi}{c}\right)\right] \tag{68a}$$

$$2\pi m^2 \sigma_{3r} = -\mu a_{0r}\frac{\partial}{\partial c}\left(\mathrm{Im}\int_0^{\infty}\left[\Delta_\Psi\Psi_0\left(\frac{z}{\xi}\right) + \Delta_\Omega\Omega_0\left(\frac{z}{\xi}\right)\right]\frac{\mathrm{d}z}{z^2(z^2-c^2)} - \frac{\pi}{2}\frac{1}{c^3}\left[R_\Psi\theta_1\left(\frac{\xi}{c}\right) + R_\Omega\frac{c}{\xi}\sqrt{\left[1-\left(\frac{c}{\xi}\right)^2\right]}\right]\right) \tag{68b}$$

where σ_{30} follows from (68b) by changing a_{0r} to a_{00} and the sign of the K-subscripted terms. In (68)

$$R = \chi(S_B + S_A), \quad R_\Psi = T_A + U_B, \quad R_\Omega = T_A + T_B \tag{69}$$

where c replaces z in the definitions (29). The non-integral terms in (68) arise to account for the pole residues at $z = c$ now appearing in the integrands. With this effect extracted, the formal c-differentiation can take place, and the integrals in (68) are now identical in form to those in (49). Thus, in view of (52), (54) and (48), (68) becomes

$$\frac{1}{b_3}\sigma_{33} = -1 + \frac{1}{2c\Phi_1}\frac{\partial \hat{c}}{\partial c}\left[\frac{R}{\alpha c^3}\theta_1\left(\frac{\xi}{c}\right)\right] \tag{70a}$$

$$\frac{1}{b_r}\sigma_{3r} = -1 + \frac{1}{2c\Phi_2}\frac{\partial \hat{c}}{\partial c}\frac{1}{c^3}\left[R_\Psi\theta_1\left(\frac{\xi}{c}\right) + R_\Omega\frac{c}{\xi}\sqrt{\left[1-\left(\frac{c}{\xi}\right)^2\right]}\right] \tag{70b}$$

for $x_3 = 0$, $cs < r < s/m$. Here $\sigma_{3\theta}$ follows from (70b) by replacing b_r with b_θ, and by changing the sign of R_Ω. For $r = cs+$, these forms give, upon differentiation, use of (50) and keeping only the singular terms, the results

$$\sigma_{33} \sim \frac{K_1}{\sqrt{(2\pi)}\sqrt{(r-cs)}}, \quad \sigma_{3r} \sim \frac{K_2}{\sqrt{(2\pi)}\sqrt{(r-cs)}}, \quad \sigma_{3\theta} \sim \frac{K_3}{\sqrt{(2\pi)}\sqrt{(r-cs)}} \tag{71}$$

where (K_1, K_2, K_3) are, respectively, the mode (I, II, III) dynamic stress intensity factors given by

$$K_1 = -\frac{\sqrt{(\pi cs)}}{\Phi_1 c^2 \alpha} Rb_3, \quad K_2 = -\frac{\sqrt{(\pi cs)}}{\Phi_2 c^2 \beta} Rb_r, \quad K_3 = -\frac{\sqrt{(\pi cs)}}{\Phi_2 c^2} m^2 \beta b_\theta \tag{72}$$

and (α, β, R) are now functions of c. At this point, we note that R is the Rayleigh function with zeroes at $\pm c_R$. Thus (72) confirms the well-known (Broberg, 1960; Brock, 1977) results that a growing crack loses its stress singularity in modes I and II at the Rayleigh wave speed, while the mode III singularity vanishes at the shear wave speed ($c = 1/m > c_R$).

Another quantity of interest is E_c, the rate per unit length of crack edge at which energy is produced by the growth of the penny-shaped crack:

$$E_c = \frac{c_1}{2\pi cs}\int (\mathbf{e}_3 \cdot \boldsymbol{\sigma} \cdot \dot{\mathbf{U}})\, \mathrm{d}A. \tag{73}$$

Here integration is over that area of the $r\theta$-plane containing the crack, while the tractions are for the *complete* solution, and are evaluated on this plane. By following the work of Achenbach (1970), (73) can be evaluated as follows: from (70) and (71) we note that the total stress field vanishes on the crack surface, but is square-root singular at $r = cs+$. Then, from (35) and (54), we see that $\dot{\mathbf{U}}$ is square-root singular at $r = cs-$, i.e.,

$$\dot{\mathbf{U}} \sim \frac{m^2}{\mu c}\left(\frac{1}{\Phi_2}b_r, \frac{1}{\Phi_2}b_\theta, \frac{1}{2\Phi_1}b_3\right)\sqrt{\left(\frac{s}{2c}\right)}\frac{1}{\sqrt{(cs-r)}}, \tag{74}$$

while, of course, vanishing for $r > cs$. This combination of singularities has the effect of a Dirac function at $r = cs$. Its sifting property can, therefore, be used in view of (71) and (74) to show that

$$E_c = \frac{\pi m^2}{8\mu c^4} c_1 s(e_r b_r^2 + e_\theta b_\theta^2 + e_3 b_3^2) \tag{75}$$

where the coefficients

$$e_r = \frac{4R}{c^2\Phi_2^2\beta}, \quad e_\theta = \frac{4m^2\beta}{\Phi_2^2}, \quad e_3 = \frac{R}{c^2\Phi_1^2\alpha} \tag{76}$$

are dimensionless constants, and (α, β, R) are again functions of c.

As could be discerned from the general result (20), and is confirmed by (54) and (71), the problem axisymmetry uncouples the solution in such a manner that the three loading

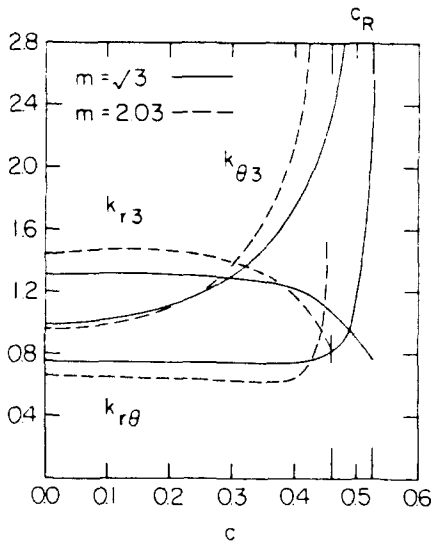

Fig. 2. Ratios of fracture mode contributions to fracture energy rate vs non-dimensionalized crack speed.

traction components are associated one-to-one with the corresponding fracture modes. In (75), therefore, one can examine the relative importance of the fracture modes to the energy rate in terms of the dimensionless ratios

$$k_{r\,\mathrm{I}} = \frac{c_r}{c_{\mathrm{II}}}, \quad k_{\mathrm{II\,I}} = \frac{c_{\mathrm{II}}}{c_{\mathrm{I}}}, \quad k_{r\mathrm{III}} = \frac{c_{\mathrm{III}}}{c_r}. \tag{77}$$

In Fig. 2 we plot these ratios vs $c < c_R$ for two values of m, and see that $(k_{\mathrm{II\,I}}, k_{r\mathrm{III}})$ are less than unity for low $(c \sim 0)$ crack speeds, but eventually increase rapidly with speed. The ratio $k_{r\,\mathrm{I}}$, however, exceeds unity for $c \sim 0$, then decreases with speed. Thus, for $b_r = b_{\mathrm{II}} = b_{\mathrm{I}}$, the mode III contribution to E_c exceeds that due to mode I at low crack speeds, and the mode I effect, in turn, exceeds that of mode III. This tendency changes, however, with crack speed and, at high speeds $(c \sim c_R)$, the mode III contribution dominates, and mode II has a stronger effect than mode I. Thus, even in an idealized problem, the relative importance of the three fracture modes in the energy of crack growth is sensitive to crack speed.

9. DISCUSSION

This paper presented an exact analysis of penny-shaped crack growth at constant speed under combined tension/in-plane shear/torsion loading. In keeping with the crack geometry, the loading variation was axisymmetric with respect to the crack center. By assuming that the loadings could be represented as polynomials in the crack plane spatial coordinates, the problem could, by superposition, be reduced to a series of problems with differing degrees of homogeneity in the spatial variables and time.

These problems were put into forms which were convenient for study, and which emphasized their basic similarity with 2D problems of plane crack growth solved exactly by Brock (1978). Thus, trial functions which required only the determination of arbitrary constant coefficient vectors were immediately identified. Nevertheless, Cauchy theorem-based manipulations of the resulting crack plane tractions were required to show that the functions indeed gave the appropriate polynomial forms on the crack itself.

The trial forms had the advantage that they were simple, that the correct singular behavior at the crack edge could be maintained by only one coefficient vector, and, above all, that they exhibited the same number of unknown coefficients as that needed to define a polynomial homogeneous to a given degree. This resulted in a set of linear algebraic equations for the unknown coefficients. One possible goal of future research might be,

therefore, to seek alternative trial forms which would lead to a strongly banded, or even diagonal, matrix for these equations.

Two specific cases—varying pure tension and uniform tension in-plane shear torsion—were worked out in some detail, in order to illustrate completion of the solution process. The latter case was also studied in terms of fracture mechanics, and the relative contributions of the three fracture modes to the fracture energy rate were found to be dependent on crack growth rate. This implies that the nature of rapid 3D crack growth under mixed-mode loading may be influenced by how fast the process occurs as well as by the loading applied.

General expressions for the displacements of a given degree of homogeneity throughout one half-space bounded by the crack plane were also given. Their forms showed an uncoupling effect also apparent in the crack plane tractions: the torsional mode of crack surface slip affects only the tangential displacement. This is, of course, an immediate consequence of the axisymmetric loading variation and the crack geometry. Indeed, it could be argued that the solution process would have been much more efficient had this axisymmetry been invoked at the beginning. For example, the Hankel transform (Sneddon, 1972) is most useful in such cases.

However, it must be emphasized here, as at the outset, that the results presented are a first-step extension; it is hoped that the general approach taken here will be more adaptable to transient 3D crack growth problems which exhibit neither axisymmetry nor lack of a characteristic length.

In closing, it should also be noted that the exact 3D solution process for the idealized transient problems presented here are not intended to supplant the numerical/approximate work currently being done in 3D dynamic crack studies. Clearly, the difficulty of non-static 3D crack problems requires the use of accurate numerical formulations in many cases. Nevertheless, it is hoped that the availability of exact transient 3D results for crack growth will prove useful, especially as a source of limit-case results.

REFERENCES

Achenbach, J. D. (1970). Extension of a crack by a shear wave. *Z. Angew. Math. Phys.* **21**(6), 887–900.

Achenbach, J. D. and Brock, L. M. (1971). Rapid extension of a crack. *J. Elasticity* **1**(1), 51–63.

Achenbach, J. D., Gautesan, A. K. and McMaken, H. (1982). *Ray Methods for Waves in Elastic Solids*. Pitman, Belfast.

Broberg, K. B. (1960). The propagation of a brittle crack. *Ark. Fys.* **18**(10), 159–192.

Brock, L. M. (1976). Non-symmetric extension of a small flaw into a plane crack at a constant rate under polynomial-form loadings. *Int. J. Engng Sci.* **14**, 181–190.

Brock, L. M. (1977). Two basic problems of plane crack extension: a unified treatment. *Int. J. Engng Sci.* **15**, 527–536.

Brock, L. M. (1978). Dynamic analysis of non-symmetric problems for frictionless indentation and plane crack extension. *J. Elasticity* **8**(3), 273–283.

Brock, L. M. (1986). A transient three dimensional analysis of non-uniform dislocation distribution growth by climb and glide over non-planar surfaces. *Proc. R. Soc. Lond.* **A407**, 299–311.

Brock, L. M. (1989). Some exact transient results for axially symmetric fracture and contact with friction. University of Kentucky College of Engineering Technical Report, December 1989.

deHoop, A. T. (1960). A modification of Cagniard's method for solving seismic pulse problems. *Appl. Scient. Res.* **B8**, 349–360.

Erguven, M. E. (1985). Running penny-shaped crack in an infinite elastic solid under torsion. *Int. J. Fracture* **29**, 135–142.

Fabrikant, V. I. (1989). *Applications of Potential Theory in Mechanics*. Kluwer Academic Publishers, Dordrecht.

Gradshteyn, I. S. and Ryzhik, I. M. (1980). *Table of Integrals, Series and Products*. Academic Press, New York.

Hadamard, J. (1908). Theorie des equations aux derivees partielles lineares hyperboliques et du probleme de Cauchy. *Acta Math.* **31**, 333–380.

Martin, P. A. and Wickham, G. R. (1983). Diffraction of elastic waves by a penny-shaped crack. *Proc. R. Soc. Lond.* **A390**, 91–129.

McCarthy, M. F. and Hayes, M. A. (eds) (1989). *Elastic Wave Propagation, Proceedings of the Second IUTAM IUPAP Symposium on Elastic Wave Propagation*. North-Holland, Amsterdam.

Panasyuk, V. V., Andrejkiv, A. E. and Stadnik, M. M. (1981). Three-dimensional static crack problem solution (a review). *Engng Fracture Mech.* **14**, 245–260.

Peirce, B. O. and Foster, R. M. (1957). *A Short Table of Integrals*, 4th edn. Blaisdell, Waltham, MA.

Rosakis, A. J., Ravi-Chandar, K. and Rajapakse, Y. (eds) (1988). *Analytical, Numerical and Experimental Aspects of Three Dimensional Fracture Processes*. AMD Vol. 91. ASME, New York.

Sneddon, I. N. (1972). *The Use of Integral Transforms*. McGraw-Hill, New York.

Willis, J. R. (1973). Self-similar problems in elastodynamics. *Phil. Trans. R. Soc. Lond.* **A274**, 435–491.